Chemistry SELECT

www.chemistryselect.org

A journal of ChemPubSoc Europe

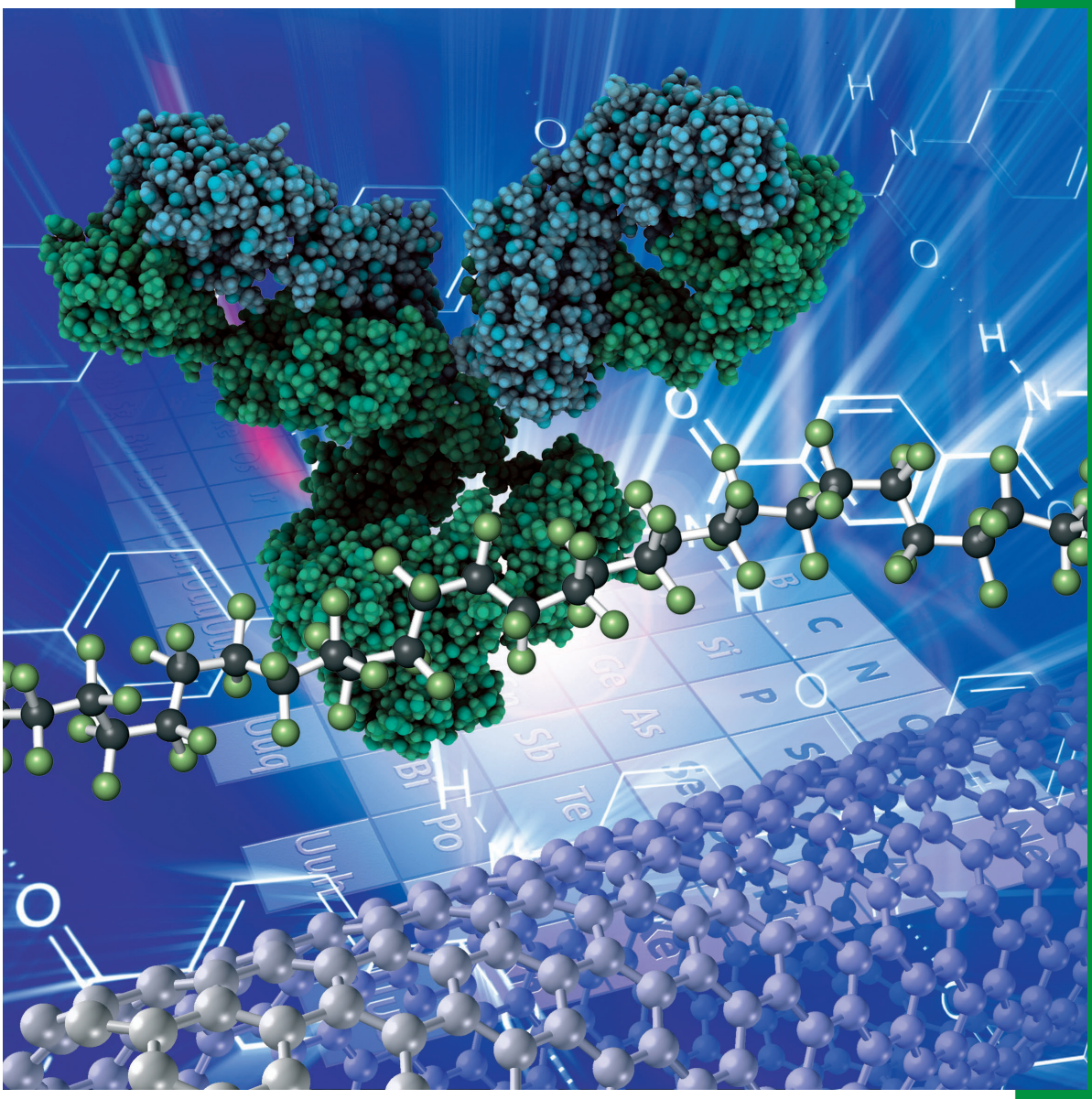

REPRINT

WILEY-VCH

ChemPubSoc Europe

DOI: 10.1002/slct.201701961

Chemistry SELECT Full Papers

Inorganic Chemistry

Synthesis, Structural Characterization and Biological Evaluation of Rhenium(I) Tricarbonyl Complexes with β-Carboline Ligands.

Iván Maisuls,[a, b] Ezequiel Wolcan,[a] Oscar E. Piro,[c] Eduardo E. Castellano,[d] Gabriela Petroselli,[e] Rosa Erra-Balsells,[e] Franco M. Cabrerizo,*[b] and Gustavo T. Ruiz*[a]

Two β-carboline rhenium(I) complexes, *fac*-[$Re(CO)_3$(dppz)(nHo)]O_3SCF_3 and *fac*-[$Re(CO)_3(nHo)_2Cl$] where dppz = dipyrido[3, 2-a:2′,3′-c] phenazine and nHo = 9H-pyrido[3, 4-b] indole (norharmane), have been synthesized. These complexes were fully characterized by structural X-ray diffraction, ^1H and ^{13}C NMR, UV-vis absorption and FT-IR spectroscopy and mass spectrometry. Ground state geometry optimization was carried out in vacuo with the PBE0 hybrid functional using the LanL2DZ basis set. The characterization was complemented with TD-DFT calculations using several hybrid functionals. Cellular uptake and cytotoxic effect of both complexes against human lung carcinoma (A549) cells were evaluated. For comparative purpose, two related *fac*-$[Re(CO)_3(L)(nHo)]^+$ complexes (L = bpy and phen) were included in the biological studies. The anti-proliferative effect of the compounds was rationalized in terms of the different extension of the ligands π-system.

Introduction

Rhenium(I) complexes comprise a group of compounds showing quite interesting physicochemical features, i.e., rich excited-state behavior,[1] thermal and photochemical stability,[2] large Stokes shift and long luminescence lifetimes.[3] These properties make them appealing candidates for diverse applications in broad research areas such as photo-induced electron transfer,[4] solar energy conversion,[5] catalysis,[6] oncology[7] and nuclear medicine,[8] among others.

In particular, due to their luminescent properties, Re(I) complexes are used as biological labelling reagents[9] and also as non-covalent luminescent molecular probes for bio-molecules and cell imaging.[10] As such, they can be easily followed in intracellular domains by conventional and/or time-resolved emission microscopy. This is appropriate to elucidate their cellular distribution and, potentially, their mechanism of action.

Rhenium(I) tri-carbonyl complexes, *fac*-$[Re(CO)_3(L_1)(L_2)]$ (where L_1 and L_2 are different mono or bidentate ligands), represent a subgroup of Re(I) complexes having a -$Re(CO)_3$ core in its architecture. This core makes them quite robust from the chemical point of view. Moreover, *fac*-$[Re(CO)_3(L_1)(L_2)]$ complexes represent versatile starting materials that can be chemically modified at ease (that is in 1–3 step synthesis) introducing specific ligands to fine-tune their physical or chemical properties.[2,11] Therefore, rhenium organometallic compounds based on the -$Re(CO)_3$ core deserve to be further investigated.

The combination of transition metals with bioactive ligands offers the possibility of designing novel compounds that may optimize or increase the intrinsic chemical, photochemical and/or pharmacological properties of the free ligands. In this context, we have undertaken the search of novel complexes based on the combination of both -$Re(CO)_3$ core and a group of alkaloids called β-carbolines (βCs) as ligands. From the chemical point of view, βCs derive from 9*H*-pyrido[3, 4-b]indole or norharmane (nHo, Scheme 1(a)). The interest in these alkaloids arises from their biological and biochemical role. In fact, βCs were found to be active compounds in several biochemical and pharmacological[12] processes. Morever, βCs have also shown quite unique and interesting photochemical,[13] photophysical and/or photosensitizing properties.[14] In consequence, the use of these alkaloids in different applications in the biomedical fields, such as photodynamic therapy, has been described.[15] Recently, we have synthesized and fully characterized two novel -$Re(CO)_3$ complexes with polypyridines and nHo as ligands.[16] Briefly, nHo binds to the metal center through the pyridine nitrogen atom. Such a kind of coordina-

[a] *I. Maisuls, Prof. E. Wolcan, Prof. G. T. Ruiz*
INIFTA
UNLP (CCT La Plata-CONICET), Diag. 113 y 64, C.C. 16, Suc. 4, (B1906ZAA) La Plata, Argentina
E-mail: gruiz@inifta.unlp.edu.ar
[b] *I. Maisuls, Prof. F. M. Cabrerizo*
IIB-INTECH – UNSAM-CONICET
I. Marino Km 8,2. CC 164, (7130) Chascomús, Buenos Aires, Argentina
E-mail: fcabrerizo@intech.gov.ar
[c] *Dr. O. E. Piro*
Instituto IFLP (CCT La Plata-CONICET) y Depto. de Física
FCE-UNLP, C.C. 67
(1900) La Plata, Argentina
[d] *Dr. E. E. Castellano*
Instituto de Física de São Carlos
USP, C.P. 369
13560 São Carlos, Brazil
[e] *Dr. G. Petroselli, Prof. R. Erra-Balsells*
CIHIDECAR-CONICET, Departamento de Química Orgánica, FCEyN UBA
Pabellón II, 3er P., Ciudad Universitaria, (1428) Buenos Aires, Argentina

Supporting information for this article is available on the WWW under https://doi.org/10.1002/slct.201701961

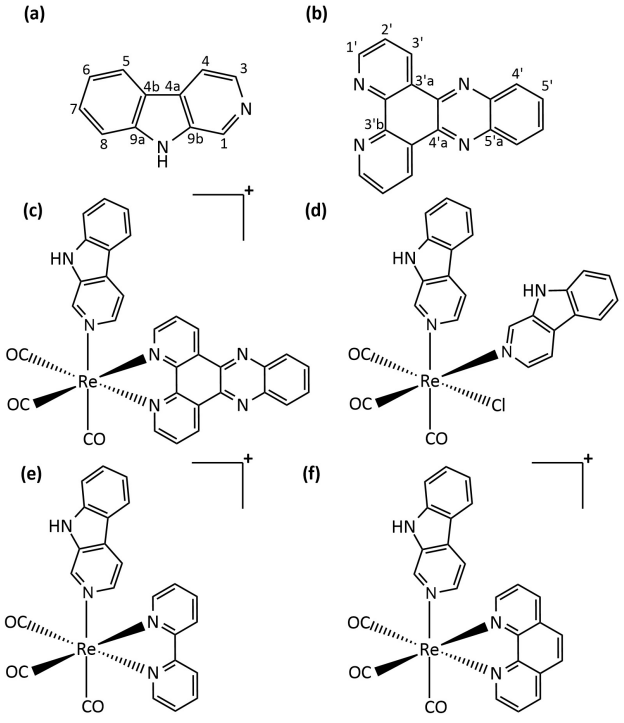

Scheme 1. Schematic structure of **(a)** norharmane, **(b)** dppz, **(c)** *fac*-[$Re(CO)_3$(dppz)(nHo)]$^+$, **(d)** *fac*-[$Re(CO)_3(nHo)_2Cl$], **(e)** *fac*-[$Re(CO)_3$(bpy)(nHo)]$^+$ and **(f)** *fac*-[$Re(CO)_3$(phen)(nHo)]$^+$.Carbons have been numbered for the NMR analysis.

tion arrangement has been referred as a good strategy for the development of novel systemic drugs based on βCs potentially having a reduced neurotoxic effects.[17]

Certainly, the search of novel -$Re(CO)_3$ complexes coordinating βCs represents an excellent alternative that deserve to be further explored. In this context, we report herein the synthesis and full characterization of two novel βC–Re(I) complexes, namely *fac*-[$Re(CO)_3$(dppz)(nHo)]$^+$, where dppz = dipyrido[3,2-a:2′,3′-c] phenazine, a known DNA intercalating molecule (Scheme 1(b)), and the first neutral Re(I) complex with only nHo as ligands, *fac*-[$Re(CO)_3(nHo)_2Cl$] (Scheme 1(c) and (d), respectively). Moreover, as a first step in the biological evaluation, the cytotoxicity activity of [$Re(CO)_3$(bpy)(nHo)]$^+$ (Scheme 1(e)), [$Re(CO)_3$(phen)(nHo)]$^+$ (Scheme 1(f)), [$Re(CO)_3$(dppz)(nHo)]$^+$ and $Re(CO)_3(nHo)_2Cl$ complexes against human carcinoma lung cells (A549) as well as their cellular uptake was investigated.

Results and Discussion

Two Re(I) complexes with nHo as ligands, *fac*-[$Re(CO)_3$(dppz)(nHo)]$^+$ and *fac*-[$Re(CO)_3(nHo)_2Cl$], were obtained and fully characterized by elemental analysis, FT-IR, NMR and by a combination of mass spectrometry techniques. Also, the solid state structure of the $Re(CO)_3(nHo)_2Cl$ complex was solved by X-ray diffraction methods.

HRESI-MS and UV-MALDI-MS

Mass spectrometry (MS) analysis was performed to determine the structure of rhenium complexes. Figure S1a shows the HRESI mass spectrum in positive ion mode of $Re(CO)_3(nHo)_2Cl$ complex (MW = 642.08). The intact molecular ion was observed as sodiated adduct $[M+Na]^+$. Contributions from ^{187}Re and ^{185}Re (62.6 and 37.4% natural abundance, respectively) can be observed at m/z values of 665.035 and 663.034. Structure diagnosis signals were obtained by MALDI-MS when DCTB and nHo were used as matrices, Figures S1b and S1c. In negative ion mode, the intact molecular ion $[M]^-$ as anion radical species was detected at m/z = 642.53 when LDI-MS was used and at m/z = 642.73 when MALDI-MS was used (matrix, nHo), Figure S2.

The HRESI mass spectrum in positive ion mode of the cationic organometallic complex [$Re(CO)_3$(dppz)(nHo)]$^+$ (MW = 720.74) is shown in Figure S3a. The intact molecular ion was observed as cation $[M]^+$ at m/z values of 721.098 and 719.095 (contributions from ^{187}Re and ^{185}Re, respectively). Additionally, the intact molecular ion for the complex was detected as cation $[M]^+$ by MALDI-MS when DCTB and nHo were used as matrices and also when no matrix was added (LDI-MS) (Figures S3b and S3c)

Structural characterization by X-ray diffraction

Figure 1 is an ORTEP[18] drawing of the $Re(CO)_3(nHo)_2Cl$ complex. Crystal data, data collection procedure, structure

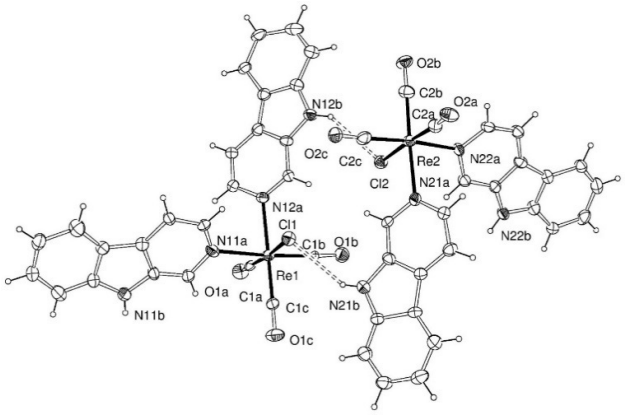

Figure 1. View of dimeric *fac*-[$Re(CO)_3(nHo)_2Cl$] complex showing the displacement ellipsoids of non-H atoms at the 30% probability level. Metal-ligand bonds are indicated by full lines and intermolecular N–H•••Cl bonds by dashed lines. For clarity, in the fused heterocyclic rings only the N-atoms have been labelled. Selected bond lengths [Å] and angles [°] around Re(I) ions: **Re1**; C(1 A)-Re(1): 1.980(15), C(1B)-Re(1): 1.923(12), C(1C)-Re(1): 1.873 (12), N(11 A)-Re(1): 2.281(14), N(12 A)-Re(1): 2.247(9), Re(1)-Cl(1): 2.483(3). **Re2**; C(2 A)-Re(2): 1.900(13), C(2B)-Re(2): 1.902(14), C(2C)-Re(2): 1.882(19), N(21 A)-Re(2): 2.208(10), N(22 A)-Re(2): 2.164(12), Re(2)-Cl(2): 2.495(3).

determination methods and refinement results are summarized in Table 1. Bond distances and angles around the metal ions are in Tables S1-S2.

Table 1. Crystal data and structure refinement results for $Re(CO)_3(nHo)_2Cl$.

Empirical formula	$C_{25}\ H_{16}\ Cl\ N_4\ O_3\ Re$
Formula weight	642.07
Temperature	293(2) K
Wavelength	0.71073 Å
Crystal system	Monoclinic
Space group	*Pc*
Unit cell dimensions	$a = 11.2840(3)$ Å $b = 10.4360(2)$ Å $c = 29.8590(8)$ Å $\beta = 91.828(1)^\circ$
Volume	3514.4(2) Å^3
Z	4
Absorption coefficient	3.557 mm^{-1}
F(000)	1240
Crystal size	0.211 x 0.068 x 0.060 mm^3
ϑ-range for data collection	1.36 to 25.25°.
Index ranges	$-13 \le h \le 13,\ 0 \le k \le 12,\ -35 \le l \le 35$
Reflections collected	21612
Independent reflections	11152 [R(int) = 0.0827]
Observed reflections [$I > 2\sigma(I)$]	9691
Completeness to $\vartheta = 25.25^\circ$	98.0%
Refinement method	Full-matrix least-squares on F^2
Data / restraints / parameters	11152 / 2 / 613
Goodness-of-fit on F^2	1.058
Final R indices[a] [$I > 2\sigma(I)$]	R1 = 0.0441, wR2 = 0.1230
R indices (all data)	R1 = 0.0484, wR2 = 0.1246
Absolute structure parameter	-0.02(1)
Largest diff. peak and hole	0.759 and −1.321 e. Å^{-3}

[a] $R_1 = \Sigma||F_o|-|F_c||/\Sigma|F_o|$, $wR_2 = [\Sigma w(|F_o|^2-|F_c|^2)^2/\Sigma w(|F_o|^2)^2]^{1/2}$

There are two closely related but independent Re(I) complexes per asymmetric unit. Assuming that the Re–Cl bonds define the axis, the molecules can be seen as an incomplete four-bladed propeller-like structure lacking the two trans blades which are replaced by CO groups. It can be envisaged that for a right-screw rotation along the Re–Cl bond, **Re1** complex has one of its NH group on the front and the other one on the rear edges of the blades, while in **Re2** complex both NH groups are on the front blades edges. Rhenium(I) ions are in slightly distorted octahedral environments, *fac*-coordinated to three carbonyl groups [Re–C bond distances in the range from 1.87(1) to 1.98(2) Å (Re1) and from 1.88(2) to 1.90(1) Å (Re2); C–Re-C bond angles in the 89.3(5)-92.1(5)° (Re1) and 89.8(5)-92.2(6)° (Re2) intervals; C–O lengths from 1.08(2) to 1.20(1) Å (Re1) and from 1.14(1) to 1.16(2) Å (Re2); Re-C–O angles are in the 177(1)-179(1)° and 175(1)-178 (1)° ranges for **Re1** and **Re2**, respectively].

Two other cis-positions are occupied by two nHo molecules acting as mono-dentate ligand through their pyridine N-atoms along their electron lone-pair lobes [Re–N bond distances of 2.28(1) and 2.247(9) Å (Re1) and 2.21(1) and 2.16(1) Å (Re2)]. The six-fold coordination is completed by a chlorine ion [Re–Cl distances of 2.483(3) Å for Re1 and 2.495(3) Å for Re2].

As expected from extended π-bonding delocalization, the nHo ligands are planar [rms deviation of non-H atoms from the best least-squares plane less than 0.024 Å]. The molecular planes subtend dihedral angles of 59.8(2)° (Re1) and 61.7(2)° (Re2) with each other and the corresponding Re(I) ions lay nearly onto their intersections.

As shown in Figure 1, the pair of complexes is arranged in the lattice as dimeric units linked through NH•••Cl bonds [N•••Cl distances of 3.29 and 3.26 Å and (N–H•••Cl) angles of 135°].

Spectroscopic characterization

FT-IR absorption spectra of the complexes showed intense bands in the 2100–1800 cm^{-1} region, which are consistent with both the facial configuration of the carbonyl ligands and with their Cs symmetry.[19] Absorption bands were attributed to the A'1, A'' and A'2 stretching modes of CO ligands in the complexes according to our previous report on similar complexes with nHo.[16] Absorption band at 3200–3300 cm^{-1} region was assigned to N–H peak of nHo ligands which has also been reported for other metal-nHo complexes.[16,20]

^{1}H- and ^{13}C-NMR spectra showed the expected signals for both nHo and dppz ligands. However, all signals were slightly shifted, with respect to the free ligands, due to their coordination with Re atom. It is noteworthy that ^{13}C-NMR spectrum of both complexes showed a signal at high fields, i.e., δ ~ 197.5 ppm ($Re(CO)_3(nHo)_2Cl$) and δ ~ 196.4 ($[Re(CO)_3(dppz)(nHo)]^+$) which were assigned to the carbonyl ligands.

The UV-vis absorption spectrum of $Re(CO)_3(nHo)_2Cl$ in MeOH solution consists of three different absorption bands, blue line in Figure 2. The first band, showing the highest molar

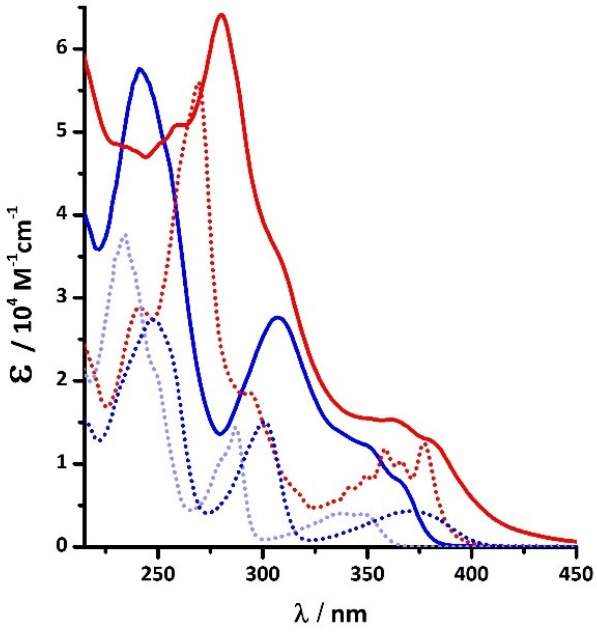

Figure 2. Absorption spectra of methanolic solution of $Re(CO)_3(nHo)_2Cl$ (blue solid line), $[Re(CO)_3(dppz)(nHo)]O_3SCF_3$ (red solid line), nHo (light blue dotted line), $nHoH^+$ (blue dotted line) and dppz (red dotted line).

absorption coefficient, ε (ε ~ 5.7 x 10^4 M^{-1} cm^{-1}), is centered at λ_{max} = 241 nm. A less intense band (ε ~ 2.8 x 10^4 M^{-1} cm^{-1}) appears at λ_{max} = 308 nm. There are two successive absorption bands appearing as shoulders of the latter band at λ_{max} ~ 348 and 365 nm (ε ~ 1.2 x 10^4 and 8.0 x 10^3 M^{-1} cm^{-1}, respectively). When comparing the absorption spectra of the complex with those recorded for free neutral (nHo) and protonated ($nHoH^+$) norharmane (light blue and blue dotted lines, respectively in Figure 2),[16,21] it is evident that, despite other electronic transitions, both nHo-like and $nHoH^+$-like βC's rings contribute, at least in part, to the overall absorption of $Re(CO)_3(nHo)_2Cl$.

This is in agreement with TD-DFT calculations discussed below. In addition, absorbance observed at λ > 300 nm also suggests the presence of new charge transfer transitions bands due to the coordination of nHo with the metal center (vide infra).

The UV-vis absorption spectrum of $[Re(CO)_3(dppz)(nHo)]O_3SCF_3$ in MeOH solutions, red line in Figure 2, consist in one intense band centered in λ_{max} = 280 nm (ε ~ 6.4 x 10^4 M^{-1} cm^{-1}) and several overlapping bands in 325–425 nm region (ε ~ 1.5 x 10^4 M^{-1} cm^{-1}), i.e. corresponding to typical vibronic components of dppz (red dotted line in Figure 2) and nHo ligands.

Theoretical calculations on $Re(CO)_3(nHo)_2Cl$

DFT and TD-DFT calculations have shed light on the nature of the absorption bands of *fac*-$[Re(CO)_3(L_1)(L_2)]$ complexes. They are comprised of a set of IL, MLCT and LMCT electronic transitions.[11c,22] In particular, these methods have been employed recently to unravel the character of the electronic transitions in $[Re(CO)_3(bpy)(nHo)]^+$.[16] Since the replacement of bpy by nHo could deeply modify the electronic structure not only of complex but also of each nHo ligand, TD-DFT calculations on $Re(CO)_3(nHo)_2Cl$ complex were performed in order to get a deeper understanding of its experimental absorption spectrum. Further, since the X-ray structure revealed that there are two un-equivalent complexes per asymmetric unit (vide supra) ground state geometry optimization was previously performed on two conformers of $Re(CO)_3(nHo)_2Cl$ (named as **Re1** and **Re2** in Figure 1).

Ground state geometry optimization

Additional structural information was obtained by DFT calculations on two **Re1** and **Re2** conformers. X-ray crystallographic data was used as reference in order to control the precision of theoretical values obtained. Tables S1-S2 show the calculations results of selected bond distances and angles for Re1 and Re2. Bond lengths and angles differed only by 0.1-0.2 Å and 3° or less showing a good agreement between data obtained by crystal structures and those obtained by computational chemistry. Self consistent field (SFC) energies in vacuo of both Re1 and Re2 conformers differed by only 0.16 Kcal/mol. Though a systematic study varying the angles between the two nHo ligands in both $Re(CO)_3(nHo)_2Cl$ conformers was not carried out, since kT ~ 0.6 Kcal/mol at 298 K, a free rotation of the nHo coordinated ligands in solution is highly probable. Under the Polarizable Continuum Model the differences in SCF energies between Re1 and Re2 were lower than 0.6 Kcal/mol.

TD-DFT calculations

TD-DFT calculations were performed on the optimized structures of Re1 and Re2 conformers. At the beginning, the relative performance of several hybrid functionals (see experimental section) was assayed by their ability to reproduce the experimental absorption spectrum in MeOH of both Re1 and Re2. The results of the simulations are shown in Figures S4a-g in comparison with the experimental absorptions. It is observed that the M06 functional gives the best agreement with the experimental absorption spectrum of $Re(CO)_3(nHo)_2Cl$ in MeOH, Figure 3.

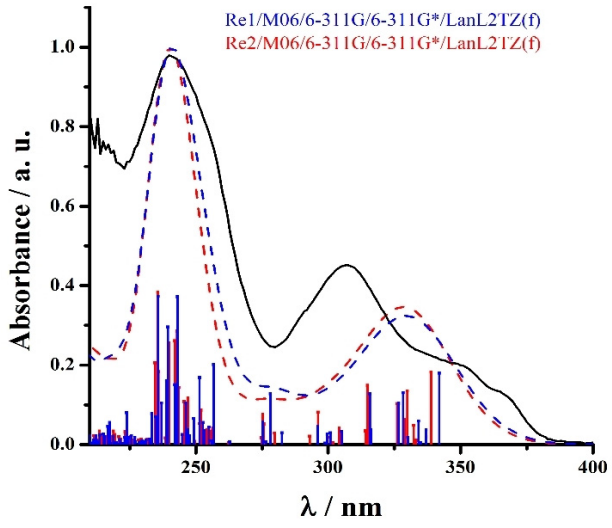

Figure 3. Comparison of the observed UV-vis absorption spectrum of $Re(CO)_3(nHo)_2Cl$ in MeOH (black curve) with TD-DFT calculated electronic transitions (vertical lines) and simulated spectra for Re1 (dashed blue curve) and Re2 (dashed red curve) under the M06/6-311G/6-311G*/LanL2TZ(f) level of theory.

Electronic transitions results calculated at the same level of theory for Re1 and Re2 in MeOH are summarized in Tables S3 and S4.

The most relevant MOs which are responsible for the electronic transitions in the absorption spectrum of $Re(CO)_3(nHo)_2Cl$ complex in the 230–400 nm wavelength range are: HOMO, LUMO, and a set of MOs H-10 through H-1 and L+1 through L+6.

By using the AOMIX program, five contributions to those MOs were considered from a Mulliken population analysis: (i) Re atom, (ii) the three carbonyls, (iii) nHo1 molecule, (iv) nHo2 molecule and (v) Cl atom. The calculated % compositions of all fragments at each MO for Re1 and Re2 in MeOH are shown in Tables S5 and S6. In the 300–400 nm region, the most relevant electronic transitions are H→L, H-1→L+1, H→L+1, H-3→L, H-4→L, H-3→L+1 and H-4→L+1. Figures 4 and S5 show the

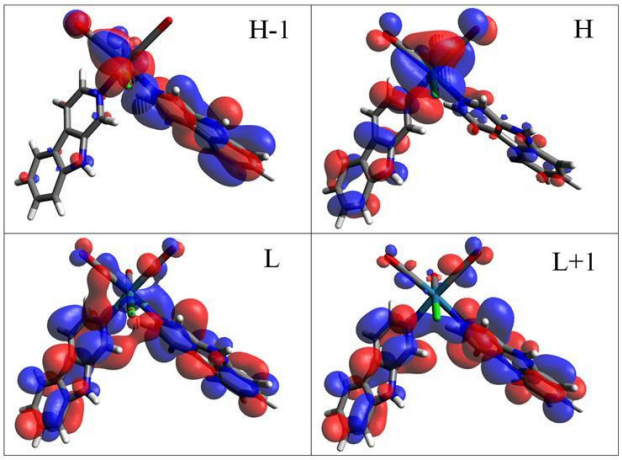

Figure 4. Spatial plots of most representative MOs in Re1 conformer of the $Re(CO)_3(nHo)_2Cl$ complex in MeOH (isovalue = 0.02).

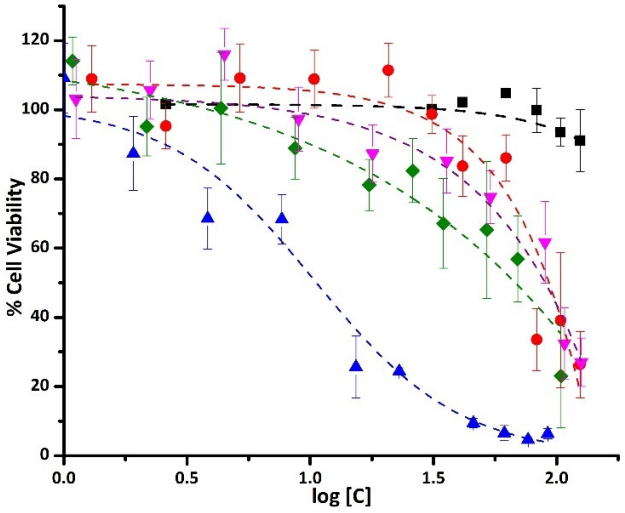

Figure 5. Cell viability of A549 cells with increasing concentrations of the four investigated complexes and nHo as control.

spatial plots of H-1, H, L and L + 1 MOs for Re1 and Re2 in MeOH, which give insight to the electronic transitions.

For Re1, Figure 4, it is observed that in MeOH H is a MO mostly centered on the Re atom (~ 43%) with smaller contributions from the three CO and nHo2 (~ 20–23%) and from nHo1 and Cl (~ 6–8%). H-1 is a MO mostly centered on nHo1 (~ 58%) with smaller contribution from the Re atom (~ 21%), the three CO and Cl (each ~ 9%) and nHo2 (~ 3%). H-3 (not shown) is a MO which is widespread between the Re atom, nHo1 and nHo2 with lesser contributions from the three CO and Cl. H-4 (not shown) is a MO mostly centered on the Re atom (~ 49%) with smaller contributions from the three CO and nHo1 (~ 22 and 17%, respectively) and from Cl (~ 9%). On the other hand, L and L + 1 are MOs centered on nHo2 and nHo1, respectively. Therefore, all the electronic transitions in MeOH in the 300–400 nm region are $MLLCT_{(Re(CO)3\rightarrow nHo1)}$ and $MLLCT_{(Re(CO)3\rightarrow nHo2)}$.

The high energy part of the spectrum, i.e., below 300 nm, is more complex and the main electronic transitions does not seem to be "pure" excitations but a mixture of nearly all of them. However, they appear to be a composition of $IL_{(nHo)}$, $LLCT_{(Cl\rightarrow nHo)}$ and $MLLCT_{(Re(CO)3\rightarrow nHo)}$ transitions. This is a distinct feature when compared to the $[Re(CO)_3(bpy)(nHo)]^+$ complex, where neat $\pi\rightarrow\pi^*$ electronic transitions centered in bpy and nHo fragments, respectively, were obtained by TD-DFT calculations.[16]

Cytotoxicity and cellular uptake of Re^I-nHo complexes

Cytotoxicity of four Re^I-nHo complexes (Scheme 1) against A549 cells was evaluated, Figure 5. Data provided herein show that the coordination of the -$Re(CO)_3$ core to nHo ligand increases the toxicity of the βC moiety to A549 cells. All the investigated complexes are more toxic than free nHo (Table 2).

Moreover, the intrinsic cytotoxicity of the complexes depends on the chemical nature of the accompanying ligand rather than on the net charge of the molecules or the nHo ligand. IC_{50} values show that the cytotoxic activity of the investigated Re^I-nHo complexes increases with the size of the ancillary or extension of the π-system of the ligands: $IC_{50}^{dppz} < IC_{50}^{phen} < IC_{50}^{bpy} < IC_{50}^{nHo}$. This accounts for the impact the chemical structure of the ligands has on the overall cytotoxicity of the investigated rhenium complexes, as it was shown for ruthenium[23] and platinum[24] complexes.

Table 2. IC_{50} of the Re^I-nHo complexes and nHo in A549 cells.

Complex	IC_{50} value (μM)
$Re(CO)_3(nHo)_2Cl$	85 ± 1
$[Re(CO)_3(bpy)(nHo)]^+$	88 ± 1
$[Re(CO)_3(phen)(nHo)]^+$	65 ± 1
$[Re(CO)_3(dppz)(nHo)]^+$	10 ± 1
nHo	> 250

The highest cytotoxicity of $[Re(CO)_3(dppz)(nHo)]^+$ might be associated to the intrinsic intercalative property of the dppz ligand with DNA (nuclear and/or mitochondrial)[25] and/or also with the differential cell penetration, which can enhance the toxicity. In fact, this complex shows a quite similar cytotoxic effect (IC_{50} = 10 μM) to the one described for cisplatin (IC_{50} = 8.0 μM) against the same cell line.[20] Therefore, is important to emphasize that $[Re(CO)_3(dppz)(nHo)]^+$ might represent an attractive alternative as a potential antitumor drug.

Re^I-nHo complexes with bpy, phen and nHo as ligands, show moderated effect on A549 cells when comparing their cytotoxicity with related metal complexes based on nHo as ligands, i.e., Ag^I-nHo and polypyridyl Ru^{II}-nHo complexes.[20,23a] Therefore, it would be interesting to study the potential use of these complexes as biological labels of intracellular domains.

Re(I)-complexes can be taken up by different types of cells. The efficiency of this process is closely related to their type of ligands and net charge.[10c] Thus, to further evaluate the uptake of this family of Re^I-nHo complexes, A549 cells were co-incubated in independent experiments and then visualized by

fluorescence microscopy by making use of the intrinsic luminescent properties (Figure S6) of these complexes. Figure 6

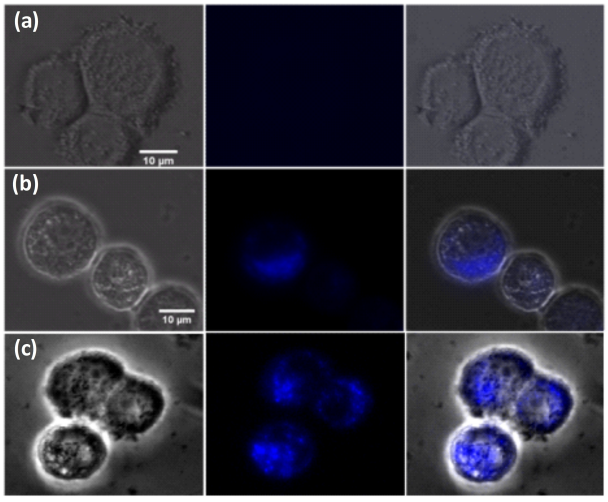

Figure 6. Phase contrast (left), fluorescence (center) and merged images (right) of **(a)** nHo (control) **(b)** $Re(CO)_3(nHo)_2Cl$ and **(c)** $[Re(CO)_3(dppz)(nHo)]^+$ of suspended A549 cells.

shows, as a representative example, images of A549 cells stained with $Re(CO)_3(nHo)_2Cl$ and $[Re(CO)_3(dppz)(nHo)]^+$. Cells are clearly stained by these types of rhenium(I) tri-carbonyl norharmane complexes. Visual inspection of the A549 cells indicated healthy cell morphology in all tested samples.

As semi-quantitative test of cell viability, cells were co-incubated with the rhenium complexes and propidium iodide, which is only taken up by dead or dying cells. Cell counting showed no evidence of damage on treated cells with respect to untreated cells as control, Figure S7. This evidences that there is no cellular death during the time (1 h) of the staining protocol (see Experimental Section).

Cells were also co-incubated with SYBR green in an attempt to elucidate the intracellular localization of $Re(CO)_3(nHo)_2Cl$, Figure 7. The absence of co-localization between both dyes suggests that the complex do not accumulate into the nucleus.

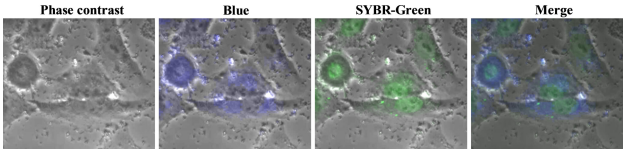

Figure 7. Attached A549 cells stained with $Re(CO)_3(nHo)_2Cl$ (Blue) and SYBR-Green.

The cellular uptake characteristics of these complexes can be estimated by their lipophilicities, which are commonly referred to as the *n*-octan-1-*ol*/water partition coefficients, expressed as *log* $P_{o/w}$.[23d] In the present study, it was not possible to estimate this parameter due to the high hydrophobicity of the complexes. This result leads us to assume that they might localize into any hydrophobic intracellular compartments such as mitochondria, lysosomes or the Golgi body, as seen in other related compounds.[26] In particular, the neutral $Re(CO)_3(nHo)_2Cl$ complex represents an excellent alternative to Re(I) complexes reported in the literature for cellular imaging or biological probes, since most of them are positively (cationic) or negatively (anionic) charged.[10c,d] Nevertheless, further studies are needed to bring light on this.

Conclusions

Two Re(I) complexes with nHo have been obtained. Solid state Structural X-ray diffraction analysis of $Re(CO)_3(nHo)_2Cl$ complex revealed that there are two closely related but independent Re(I) complexes per asymmetric unit in the crystal lattice. The molecules of each complex differed in the orientation of both NH groups of the nHo ligands. The pair of complexes is arranged in the lattice as dimeric units linked through NH•••Cl bonds. Ground state geometry optimization by DFT calculations showed that in solution the nHo ligands may rotate freely. TD-DFT calculations established that the most important electronic transitions present in the spectrum of the $Re(CO)_3(nHo)_2Cl$ complex are $MLLCT_{(Re(CO)3\rightarrow nHo1,\ nHo2)}$ along with a mixture of $IL_{(nHo)}$ and $LLCT_{(Cl\rightarrow nHo)}$ transitions.

Data reported herein show that this group of complexes allows for a great deal of structure and chemical variability, and can be fine-tuned to meet the requirements of a wide range of biological applications (fluorescence markers and/or antitumor drugs) that deserve to be further investigated. Moreover, their relatively high hydrophobicity makes these complexes suitable for micelle-based drug delivery.[27]

Supplementary Information Available

Additional computational details. General experimental procedures. Mass spectra (ESI, LDI and MALDI) of the complexes (Figs. S1, S2 and S3). Comparison of the experimental UV-vis absorption spectrum with TD-DFT calculated electronic transitions under different levels of theory (Figs. S4a-g). Spatial plots of MOs in Re2 conformer (Fig. S5). Emission spectra of the rhenium complexes (Fig. S6). Cells stained with Propidium Iodide (Fig. S7). FTIR spectra of $Re(CO)_3(nHo)_2Cl$ and $[Re(CO)_3(dppz)(nHo)]O_3SCF_3$ (Figs. S8a-b). ^1H NMR and ^{13}C NMR spectra of $Re(CO)_3(nHo)_2Cl$ and $[Re(CO)_3(dppz)(nHo)]O_3SCF_3$ (Figs. S9 and S10). Bond lengths and angles (Tables S1 and S2). TD-DFT calculations in MeOH (Tables S3 and S4). HOMOs and LUMOs compositions (Tables S5 and S6). Full bond lengths and angles (Table S7). Atomic coordinates and isotropic displacement of the non-H atoms (Table S8). Atomic anisotropic displacement parameters (Table S9). Hydrogen coordinates and isotropic displacement parameters (Table S10).

Acknowledgements

This work was supported by CONICET (PIP 0072CO), ANPCyT (PICT 2012-0423 and PICT 2012-0888), UBA X 0055BA and UNLP 11X/611 of Argentina and by FAPESP of Brazil. IM and GTR thank Dr. Croce (INIFTA, UNLP, Argentina) for their assistance in FT-IR measurements. The Ultraflex II (Bruker) TOF/TOF mass spectrometer was supported by a grant from ANPCyT (PME 125). IM thanks ANPCyT for research scholarships. E. W, O. E. P, G. P., R. E-B, F. M. C. and G. T. R. are research members of CONICET. Authors also thank Dr. M. L. Alomar for her contribution on cell imaging.

Conflict of Interest

The authors declare no conflict of interest.

Keywords: Antitumor agent · Bioinorganic chemistry · Cytotoxicity · Rhenium tricarbonyl complexes · Structure elucidation

[1] A. Vičck Jr, *Top. Organomet. Chem.* **2010**, *29*, 73–114.
[2] A. Kumar, S.-S. Sun, A. J. Lees, *Top. Organomet. Chem.* **2010**, *29*, 1–35.
[3] V. Balzani, A. Juris, M. Venturi, S. Campagna, S. Serroni, *Chem. Rev.* **1996**, *96*, 759–834.
[4] M. A. Fox, M. Chanon, *Photoinduced Electron Transfer.* Elsevier: Amsterdam **1988**.
[5] a) M. Grätzel, *Energy Resources Through Photochemistry and Catalysis.* Academic Press: New York, **1983**; b) C. G. Garcia, F. L. Jailson, Y. Neyde, I. Murakami, *Coord. Chem. Rev.* **2000**, *196*, 219–247.
[6] Y. Kuninobu, K Takai, *Chem. Rev.* **2011**, *111*, 1938–1953.
[7] a) A. Kast, S. Dieckmann, K. Wähler, T. Völker, L. Kastl, A. L. Merkel, A. Vultur, B. Shannan, K. Harms, M. Ocker, W. J. Parak, M. Herlyn, E. Meggers, *ChemMedChem.* **2013**, *8*, 924–927; b) A. Leonidova, G. Gasser, *ACS Chem. Biol.* **2014**, *9*(10), 2180–2193.
[8] a) C. Müller, C. Dumas, U. Hoffmann, P. A. Schubiger, R. Schibli, *J. Organomet. Chem.* **2004**, *689*, 4712–4721; b) K. Hashimoto, K. Yoshihara, *Top. Curr. Chem.* **2005**, *176*, 275–291; c) R. Schibli, K. V. Katti, W. A. Volkert, C. L. Barnes, *Inorg. Chem.* **2001**, *40*, 2358–2362.
[9] L. Wei, J. Babich, J. Zubieta, *Inorg. Chim. Acta* **2005**, *358*, 3691–3700.
[10] a) A. J. Amoroso, M. P. Coogan, J. E. Dunne, V. Fernandez-Moreira, J. B. Hess, A. J. Hayes, D. Lloyd, C. Millet, S. J. A. Pope, C. Williams, *Chem. Commun.* **2007**, *30*, 3066–3068; b) F. L. Thorp-Greenwood, M. P. Coogan, L. Mishra, N. Kumari, G. Rai, S. Saripella, *New J. Chem.* **2012**, *36*, 1–180; c) V. Fernández-Moreira, F. L. Thorp-Greenwood, A. J. Amoroso, J. Cable, J. B. Court, V. Gray, A. J. Hayes, R. L. Jenkins, B. M. Kariuki, D. Lloyd, C. O. Millet, C. Ff. Williams, M. P. Coogan, *Org. Biomol. Chem.* **2010**, *8*, 3888–3901; d) R. G. Balasingham, F. L. Thorp-Greenwood, C. F. Williams, M. P. Coogan, S. J. A. Pope, *Inorg. Chem.* **2012**, *51*, 1419–1426; e) V. Fernandez-Moreira, F. L. Thorp-Greenwood, M. P. Coogan, *Chem. Commun.* **2009**, *46*, 186–202.
[11] a) M. Kaplanis, G. Stamatakis, V. D. Papakonstantinou, M. Paravatou-Petsotas, C. A. Demopoulos, C. A. Mitsopoulou, *J. Inorg. Biochem.* **2014**, *135*, 1–9; b) B. S. Uppal, R. K. Booth, N. Ali, C. Lockwood, C. R. Rice, P. I. P. Elliott, *Dalton Trans.* **2011**, *40*, 7610; c) H. H. Martinez Saavedra, F. Ragone, G. T. Ruiz, P. M. David-Gara, E. Wolcan, *J. Phys. Chem. A.* **2014**, *118*, 9661–9674; d) H. H. Martinez Saavedra, C. A. Franca, G. Petroselli, R. Erra-Balsells, G. T. Ruiz, E. Wolcan, *J. Organomet. Chem.* **2013**, *745*, 470–478; e) F. Ragone, H. H. Martinez Saavedra, P. M. David-Gara, G. T. Ruiz, E. Wolcan, *J.Phys. Chem. A* **2013**, *117*, 4428–4435; f) F. Ragone, G. T. Ruiz, O. E. Piro, G. A. Etcheverría, F. M. Cabrerizo, G. Petroselli, R. Erra-Balsells, K. Hiraoka, F. S. García Einschlag, E. Wolcan, *Eur. J. Med. Chem.* **2012**, *30*, 4801–4810; g) M. R. Féliz, F. Rodriguez-Nieto, G. T. Ruiz, E. Wolcan, *J. Photochem. Photobiol., A.* **1998**, *117*, 185–192; h) G. Torchia, J. Tocho, O. E. Piro, M. P. Juliarena, G. T. Ruiz, E. Wolcan, M. R. Féliz, *Dalton Trans.* **2002**, 2194–2202.
[12] a) M. L. Alomar, F. A. O. Rasse-Souriani, A. Gamuza, V. M. Cóceres, F. M. Cabrerizo, S. O. Angel, *BMC Res. Notes* **2013**, *6*, 1–6 ; b) R. Cao, H. Chen, W. Peng, Y. Ma, X. Hou, H. Guan, X. Liu, A. Xu, *Eur. J. Med. Chem.* **2005**, *40*, 991–1001; c) M. G. Olmedo, L. Cerioni, M. M. González, F. M. Cabrerizo, V. A. Rapisarda, S. I. Volentini, *Food Microbiol.* **2017**, *62*, 9–14; d) G. M. Olmedo, L. Cerioni, M. M. González, F. M. Cabrerizo, S. I. Volentini, V. A. Rapisarda, *Front. Microbiol.* **2017**, *8*, 347; e) R. Cao, W. Peng, Z. Wang, A. Xu, *Curr. Med. Chem.* **2007**, *14*, 479–500.
[13] a) M. M. Gonzalez, M. L. Salum, Y. Gholipour, F. M. Cabrerizo, R. Erra-Balsells, *Photochem. Photobiol. Sci.* **2009**, *8*, 1139–1149; b) M. M. Gonzalez, J. Arnbjerg, M. P. Denofrio, R. Erra-Balsells, P. R. Ogilby, F. M. Cabrerizo, *J. Phys. Chem. A* **2009**, *113*, 6648–6656; c) F. M. Cabrerizo, J. Arnbjerg, M. P. Denofrio, R. Erra-Balsells, P. R. Ogilby, *ChemPhysChem.* **2010**, *11*, 796–798; d) F. A. O. Rasse-Souriani, M. P. Denofrio, J. G. Yañuk, M. M. Gonzalez, E. Wolcan, M. Seifermann, R. Erra-Balsells, F. M. Cabrerizo, *Phys. Chem. Chem. Phys.* **2016**, *18*, 886–900.
[14] a) M. Vignoni, R. Erra-Balsells, B. Epe, F. M. Cabrerizo, *J. Photochem. Photobiol., B.* **2014**, *132*, 66–71; b) M. M. Gonzalez, M. Vignoni, M. Pellon-Maison, M. A. Ales-Gandolfo, M. R. Gonzalez-Baró, R. Erra-Balsells, B. Epe, F. M. Cabrerizo, *Org. Biomol. Chem.* **2012**, *10*, 1807–1819; c) M. M. Gonzalez, F. A. O. Rasse-Souriani, C. A. Franca, R. Pis Diez, Y. Gholipour, H. Nonami, R. Erra-Balsells, F. M. Cabrerizo, *Org. Biomol. Chem.* **2012**, *10*, 9359–9372; d) H. Guan, X. Liu, W. Peng, R. Cao, Y. Ma, H. Chen, A. Xu, *Biochem. Biophys. Res. Commun.* **2006**, *342*, 894–901; e) M. M. Gonzalez, M. Pellon-Maison, M. A. Ales-Gandolfo, M. R. Gonzalez-Baró, R. Erra-Balsells, F. M. Cabrerizo, *Org. Biomol. Chem.* **2010**, *8*, 2543–2552; f) M. Vignoni, F. A. O. Rasse-Souriani, K. Butzbach, R. Erra-Balsells, B. Epe, F. M. Cabrerizo, *Org. Biomol. Chem.* **2013**, *11*, 5300–5309.
[15] F. A. O. Rasse-Souriani, K. Butzbach, M. M. Gonzalez, F. M. Cabrerizo, B. Epe, *Photochem. Photobiol.* **2016**, *92*, 611–619.
[16] I. Maisuls, E. Wolcan, O. E. Piro, G. A. Etcheverría, R. Erra-Balsells, G. Petroselli, F. M. Cabrerizo, G. T. Ruiz, *Dalton Trans.* **2015**, *44*, 17064–17074.
[17] D. A. Gearhart, E. J. Neafsey, M. A. Collins, *Neurochem. Int.* **2002**, *40*, 611–620.
[18] L. J. Farrugia, *J. Appl. Crystallogr.* **1997**, *30*, 565.
[19] U. N. Fagioli, F. S. Garcia Einschlag, C. J. Cobos, G. T. Ruiz, M. R Féliz, E. Wolcan, *J. Phys. Chem. A.* **2011**, *115*, 10979–10987.
[20] R. A. Khan, K. Al-Farhan, A. de Almeida, A. Alsalme, A. Casini, M. Ghazzali, J. Reedijk, *J .Inorg. Biochem.* **2014**, *140*, 1–5.
[21] O. I. Tarzi, M. A. Ponce, F. M. Cabrerizo, S. M. Bonesi, R. Erra-Balsells, *ARKIVOC* **2005**, *12*, 295–310.
[22] a) A. Vlček Jr, S. Zális, *Coord. Chem. Rev.* **2007**, *251*, 258–287; b) S. Zális, A. El-Nahhas, A. M. Blanco-Rodriguez, R. M. Van der Veen, Vlček Jr, *Inorg. Chem.* **2013**, *52 (10)*, 5775–5785.
[23] a) C. Tan, S. Wu, S. Lai, M. Wang, Y. Chen, L. Zhou, Y. Zhu, W. Lian, W. Peng, L. Ji, A. Xu, *Dalton Trans.* **2011**, *40*, 8611; b) Y. Chen, M.-Y. Qin, L. Wang, H. Chao, L.-N. Ji, A. Xu, *Eur. J. Med. Chem.* **2013**, *70*, 120–129; c) U. Schatzschneider, J. Niesel, I. Ott, R. Gust, H. Alborzinia, S. Wölfl, *ChemMedChem.* **2008**, *3*, 1104–1109; d) C. A. Puckett, J. K. Barton, *J. Am. Chem. Soc.* **2007**, *129*, 46–47.
[24] A. Ghezzi, M. Aceto, C. Cassino, E. Gabano, D. Osella, *J. Inorg. Biochem.* **2004**, *98*, 73–78.
[25] G. T. Ruiz, M. P. Juliarena, R. O. Lezna, E. Wolcan, M. R. Feliz, G. Ferraudi, *Dalton Trans.* **2007**, *20*, 2020–2029.
[26] R. G. Balasingham, M. P. Coogan, F. L. Thorp-Greenwood, *Dalton Trans.* **2011**, *40*, 11663–11674.
[27] P. J. Photos, L. Bacakova, B. Discher, F. S. Bates, D. E. Discher, *J. Controlled Release.* **2003**, *90*, 323–334.
[28] C. Tan, S. Lai, S. Wu, S. Hu, L. Zhou, Y. Chen, M. Wang, Y. Zhu, W. Lian, W. Peng, L. Ji, A. Xu, *J. Med. Chem.* **2010**, *53*, 7613–7624.

Submitted: August 25, 2017
Revised: September 12, 2017
Accepted: September 14, 2017